Bioorganic & Medicinal Chemistry 17 (2009) 2282–2289

Contents lists available at ScienceDirect

Bioorganic & Medicinal Chemistry

journal homepage: www.elsevier.com/locate/bmc

Total synthesis and biological evaluation of novel C2–C6 region analogues of dictyostatin

Ian Paterson [a,*], Nicola M. Gardner [a], Esther Guzmán [b], Amy E. Wright [b]

[a] University Chemical Laboratory, Lensfield Road, Cambridge CB2 1EW, UK
[b] Harbor Branch Oceanographic Institute at Florida Atlantic University, 5600 US 1 North, Fort Pierce, FL 34946, USA

ARTICLE INFO

Article history:
Received 28 March 2008
Revised 12 June 2008
Accepted 31 October 2008
Available online 5 November 2008

Keywords:
Macrolide
Antitumour
Tubulin
Total synthesis

ABSTRACT

By exploiting a Still–Gennari HWE coupling with a common C11–C26 aldehyde, a series of C2–C6 modified analogues of the microtubule-stabilising marine natural product dictyostatin were synthesised and evaluated in vitro for growth inhibition against a range of human cancer cell lines, including the (P-glycoprotein efflux-mediated) Taxol-resistant NCI/ADR cell line. Removal of the C6 methyl substituent in dictyostatin was found to be well tolerated and led to the retention of antiproliferative activity in the low nanomolar range (IC_{50} = 43 nM in the NCI/ADR cell line), while partial and full saturation of the (2*Z*,4*E*)-dienoate region led to a progressive reduction in biological potency. The lactone ring size was found to be critical, as C21 to C19 translactonisation to afford 20-membered isodictyostatin analogues led to a significant loss of cytotoxicity. In a series of incubatory experiments performed on the PANC-1 cell line, all three of the 22-membered macrolide analogues acted in an analogous fashion to dictyostatin, through a mechanism of microtubule stabilization, causing both an accumulation of cells at the G2/M phase and formation of characteristic dense intracellular microtubule bundles.

1. Introduction

The tubulin/microtubule system is an important target in current cytotoxic chemotherapy.[1] Taxol® (**1**, Fig. 1) and its semi-synthetic derivative Taxotere® act by stabilising cellular microtubules and suppressing microtubule dynamics in cell division, and are widely used in the treatment of breast, ovarian and lung cancers. Despite the clinical utility of the taxane class of microtubule-stabilising agents, they have limited effectiveness towards multidrug-resistant cancers. Over the past decade, various structurally diverse natural products that are functionally similar to Taxol have emerged as important leads for anticancer drug discovery programmes to circumvent resistance in chemotherapy.[2] Notably, Ixempra® (**2**), a semi-synthetic lactam derivative of the bacterial natural product epothilone B (**3**), received approval by the FDA in 2007 as a new microtubule-stabilising drug for the treatment of advanced breast cancer.[3]

In a similar manner to Taxol and the epothilones, the antimitotic marine natural product dictyostatin (**4**) functions by microtubule stabilisation and G2/M arrest.[4–6] Following its re-isolation from a Caribbean deep-sea sponge by Wright and co-workers,[5] detailed NMR analysis led in 2004 to the assignment of the full stereochemistry.[6] Concurrent total synthesis efforts, as reported independently by the Paterson[7a] and Curran groups,[7b,7c] confirmed this structure and facilitated more extensive biological evaluation of this promising anticancer agent,[8] as well as the initiation of SAR studies.[9] Dictyostatin displays enhanced antiproliferative activity relative to Taxol against a range of human cancer cell lines, including multidrug-resistant cells, and binds to the taxoid binding site on β-tubulin.[8] As a conformationally constrained macrolide, dictyostatin represents an attractive template for the optimisation of a new structural class of microtubule-stabilising agent. Following extensive NMR studies and molecular modelling, the bioactive conformation of dictyostatin bound to microtubules was recently disclosed,[10] providing a promising tool for analogue design. Furthermore, the large body of available SAR data for the structurally related microtubule-stabilising agent discodermolide (**5**) also offers a useful starting point for identifying active dictyostatin analogues.[11] Notably, dictyostatin represents a naturally evolved analogue of discodermolide, that has significantly enhanced biological potency. With the goal of identifying a simplified structure with a cytotoxicity profile comparable to that of the parent natural product, we now describe in full[12] the total synthesis of a novel series of C2–C6 modified dictyostatin analogues (Fig. 2)—6-desmethyl- (**6**), 2,3-dihydro- (**7**) and 2,3,4,5-tetrahydro-dictyostatin (**8**)—and evaluate their growth inhibition against a range of human cancer cell lines, including the Taxol-resistant NCI/ADR ovarian cell line.

* Corresponding author. Tel.: +44 1223 336407; fax: +44 1223 336362.
E-mail address: ip100@cam.ac.uk (I. Paterson).

0968-0896/$ - see front matter © 2008 Elsevier Ltd. All rights reserved.
doi:10.1016/j.bmc.2008.10.084

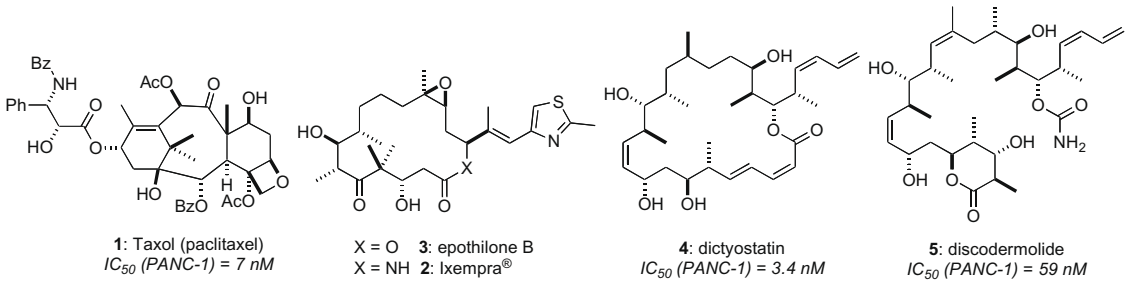

Figure 1. Structures of representative microtubule-stabilising natural products and IC_{50} data in the PANC-1 pancreatic cancer cell line.

2. Results and discussion

2.1. Synthesis of 6-desmethyldictyostatin

In previous SAR work on dictyostatin, the importance of the C16 methyl substituent was probed through the synthesis of 16-desmethyldictyostatin (**9**, Fig. 2).[9a,9b] Our biological results[9a] for **9** (IC_{50} = 130 nM in PANC-1, 1500 nM in NCI/ADR) led us to conclude that the C16 methyl group was both important in contributing to the low nanomolar levels of cytotoxicity of dictyostatin and permitting its circumvention of P-glycoprotein-mediated drug resistance. These conclusions are consistent with results from docking the bioactive conformation of dictyostatin into its β-tubulin binding site (Fig. 3),[10] where the C16 methyl group is predicted to occupy a small localised binding pocket. Looking towards achieving further structural simplifications on dictyostatin, the docking studies indicated that the C6 methyl substituent appears to be in a less important region for binding relative to that of the C16 methyl group. Hence, it was proposed to explore the contribution of the C2–C6 region to the pharmacophore by first synthesising 6-desmethyldictyostatin (**6**) to evaluate its overall cytotoxicity in a panel of Taxol-sensitive and resistant cell lines.

Access to the targeted 6-desmethyl analogue **6** was planned by adapting our existing synthetic strategy for dictyostatin[7a] and that followed for preparing an initial set of analogues[9a] (Scheme 1). This relies on a pivotal Still–Gennari HWE fragment coupling with the fully elaborated C11–C26 aldehyde **10**, followed in turn by introduction of the (2*Z*,4*E*)-dienoate by a Stille coupling with stannane **11** and Yamaguchi macrolactonisation. By pursuing a similar strategy, the primary modification required to assemble 6-desmethyldictyostatin was envisaged to be the preparation of the novel C4–C10 phosphonate **12**, lacking a C6 methyl substituent and having a PMB ether[9a] at C7 (rather than the TBS ether used initially[7a]).

Preparation of the β-ketophosphonate **12** required for the Still–Gennari fragment coupling started out from the racemic epoxide **13** (Scheme 2).[13] Using the (*S*,*S*)-Co-Salen catalyst **14**,[14] a Jacobsen hydrolytic kinetic resolution reaction afforded the (*S*)-epoxide, which was subjected to CuCl-catalysed ring opening with vinyl magnesium bromide to give the secondary alcohol **15** in 99% ee.[15] Following PMB ether formation, a sequence of oxidative olefin

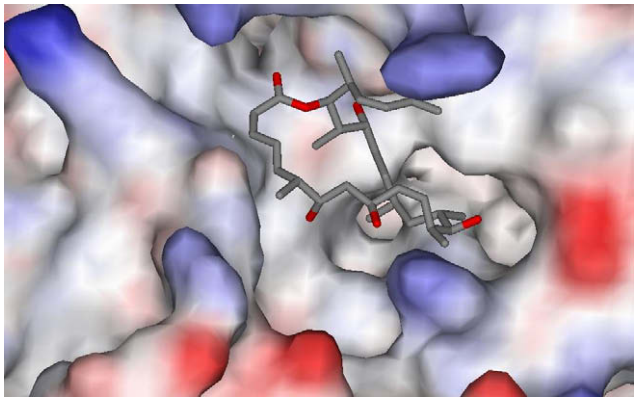

Figure 3. Dictyostatin docked into the taxoid binding site on β-tubulin.

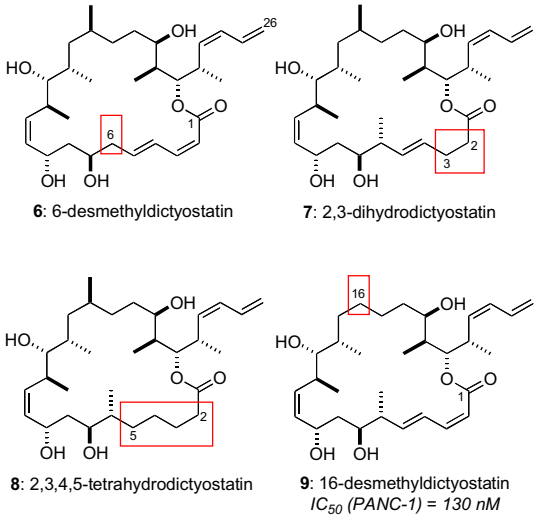

Figure 2. Structures of dictyostatin analogues **6**–**9**.

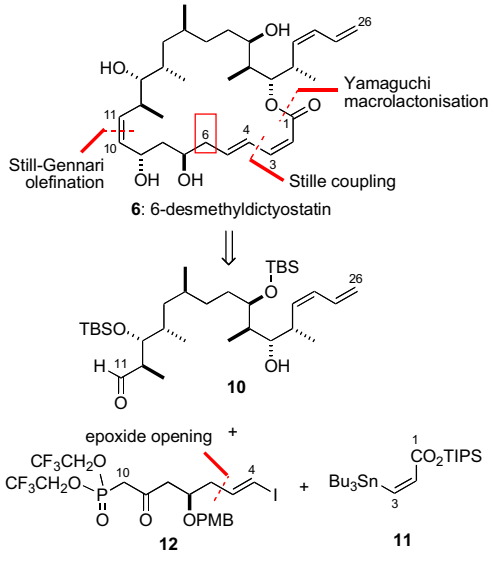

Scheme 1. Retrosynthetic analysis of 6-desmethyldictyostatin (**6**).

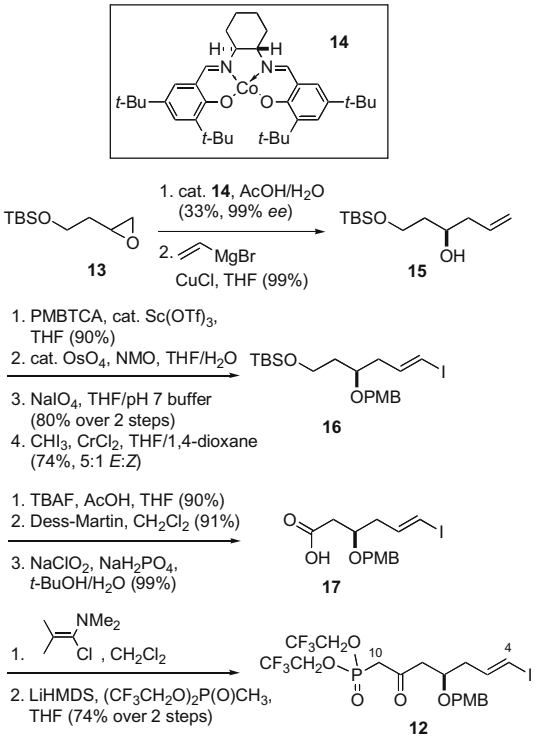

Scheme 2. Synthesis of the C4–C10 β-ketophosphonate **12**.

cleavage (OsO_4, NMO; $NaIO_4$) and Takai olefination[16] of the resulting aldehyde afforded the (*E*)-vinyl iodide **16** (53% from **15**). After TBS ether cleavage (TBAF, AcOH), the resulting alcohol was converted via the carboxylic acid **17** into the acid chloride using the Ghosez chloroenamine reagent,[17] followed by the addition of $(CF_3CH_2O)_2P(O)CH_2Li$ to provide the β-ketophosphonate **12** (60% from **16**).

As deployed in our dictyostatin total synthesis, we were now ready to perform the Still–Gennari HWE coupling[18] with the C11–C26 aldehyde **10** (Scheme 3).[7a] Following treatment of a mixture of phosphonate **12** and aldehyde **10** with K_2CO_3 (18-crown-6, PhMe, HMPA), the required (*Z*)-enone **18** was obtained in an isolated yield of 54% (3:1 *Z*:*E*). Oxidative cleavage (DDQ, pH 7 buffer) of the PMB ether in **18** then released the β-hydroxyketone in readiness for a hydroxyl-directed reduction. Reduction with $NaBH(OAc)_3$[19] afforded the expected 1,3-*anti* diol **19** with moderate selectivity (78%, 80:20 dr). Interestingly, a switch to the Corey–Bakshi–Shibata (*R*)-oxazoborolidine-mediated reduction[9f,20] gave the 1,3-*anti* diol **19** (76%, 89:11 dr) with improved levels of diastereoselectivity. After formation of the acetonide **20** ($Me_2C(OMe)_2$, PPTS), a CuTC-mediated Liebeskind–Stille coupling[21] with the vinyl stannane **11**[7a] installed the (2*Z*,4*E*)-dienoate and a Yamaguchi macrolactonisation[22] then gave the 22-membered macrolide **21**. Following global deprotection of **21** with HF·pyridine and HPLC purification, 6-desmethyldictyostatin (**6**) was isolated in 53% yield in readiness for biological testing.

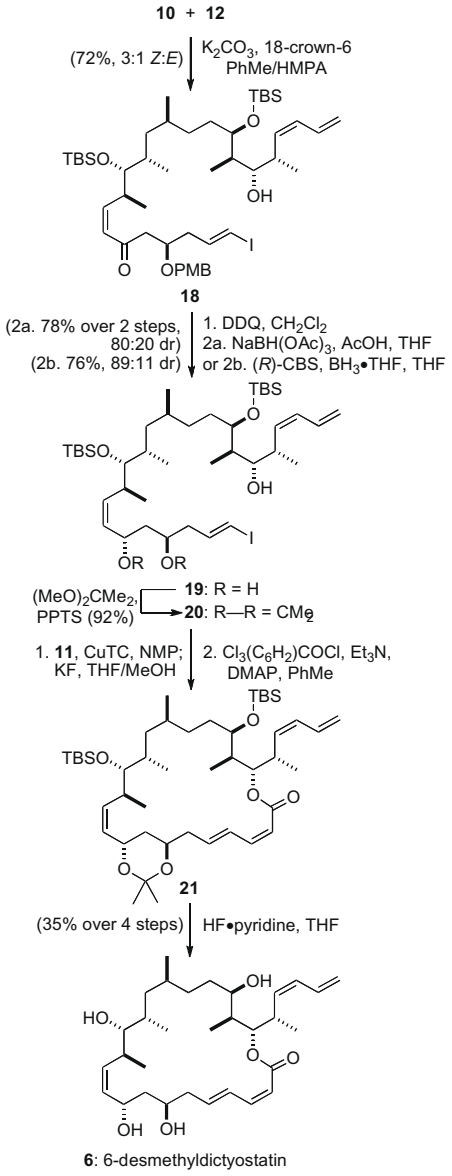

Scheme 3. Completion of the synthesis of 6-desmethyldictyostatin (**6**).

2.2. Synthesis of 2,3-dihydro- and 2,3,4,5-tetrahydrodictyostatin

The remarkable structural and stereochemical homology between the C8–C26 region of dictyostatin and the corresponding C6–C24 region of discodermolide has previously been exploited in the design of novel dictyostatin analogues[9] and hybrid molecules.[9d,9f] In contrast, the discodermolide structure features a δ-lactone in the C1–C5 region, whereas the dictyostatin macrolide differs in having a (2*Z*,4*E*)-dienoate moiety. Examination of these

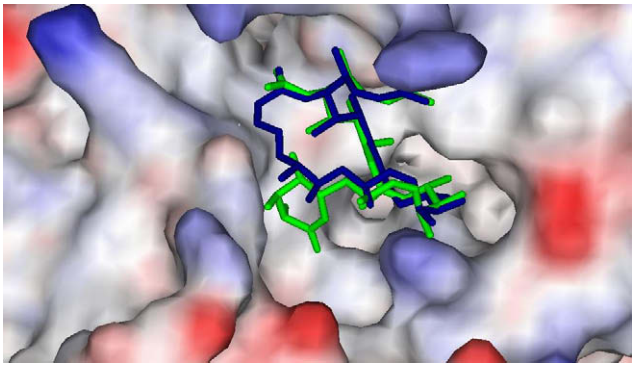

Figure 4. Dictyostatin (blue) and discodermolide (green) docked into the taxoid binding site on β-tubulin.

two natural products docked[10] into their putative common binding site on β-tubulin (Fig. 4) reveals the dictyostatin dienoate domain occupies a space that appears to be vacant for discodermolide. Hence, it was proposed to further probe the SAR associated with

the unique C1–C5 region of dictyostatin through the total synthesis of two novel reduced analogues, 2,3-dihydro- (**7**) and 2,3,4,5-tetrahydrodictyostatin (**8**).[23]

In designing a synthetic route to analogues **7** and **8**, it was apparent that removal of the dienoate negated the requirement for the Stille coupling step and hence the presence of a vinyl iodide in the β-ketophosphonate fragment. By retaining the Yamaguchi macrolactonisation and Still–Gennari HWE olefination with the pivotal aldehyde **10**, a unified route was planned to the phosphonates **22** and **23**, which differed only in the presence or absence of a $\Delta^{4,5}$-olefin, as required for the construction of analogues **7** and **8**, respectively (Scheme 4). It was envisaged that the key C1–C10 building block **22** might arise from a cross-metathesis reaction between β-ketophosphonate **24** and the simple olefin **25**. This sequence was viewed as particularly attractive due to its enhanced convergence and versatility.

Starting from the previously reported PMB ether **26**[9a] obtained using a Brown crotylation sequence, treatment with Jones reagent[24] (CrO_3, H_2SO_4) led to cleavage of the TBS ether and subsequent oxidation of the resulting alcohol to provide the acid **27** in 88% yield (Scheme 5). Conversion to the acid chloride was now possible using oxalyl chloride, and addition of $(CF_3CH_2O)_2P(O)$-CH_2Li provided the β-ketophosphonate **24** (65% from **27**) in readiness for the planned cross-metathesis reaction[25] with the terminal olefin **25**. Only when the Grubbs second-generation Ru catalyst (10 mol%) was used in the presence of AcOH[26] (10 mol%) did this afford the desired unsaturated phosphonate **22** in high yield (81%, 10:1 *E*:*Z*).[27] Raney nickel catalysed hydrogenation of alkene **22** then gave the corresponding saturated phosphonate **23** (89%), as required for the construction of 2,3,4,5-tetrahydrodictyostatin.

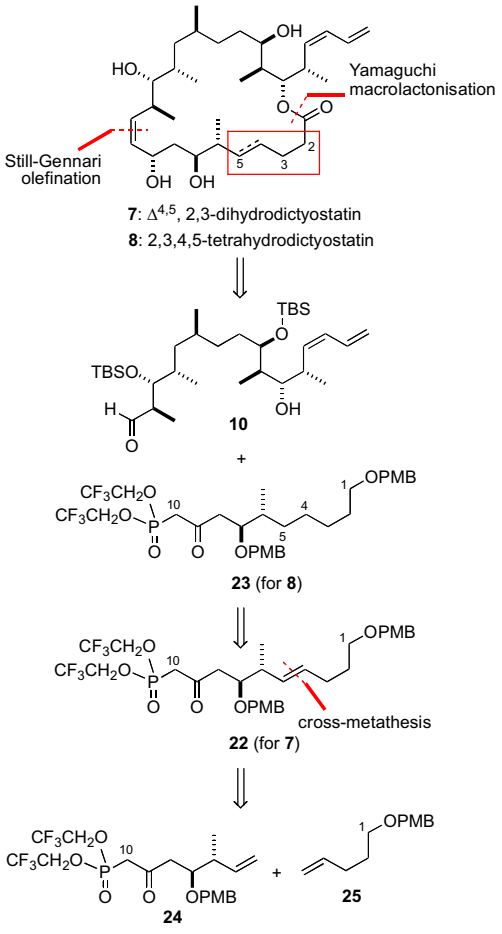

Scheme 4. Retrosynthetic analysis of dictyostatin analogues **7** and **8**.

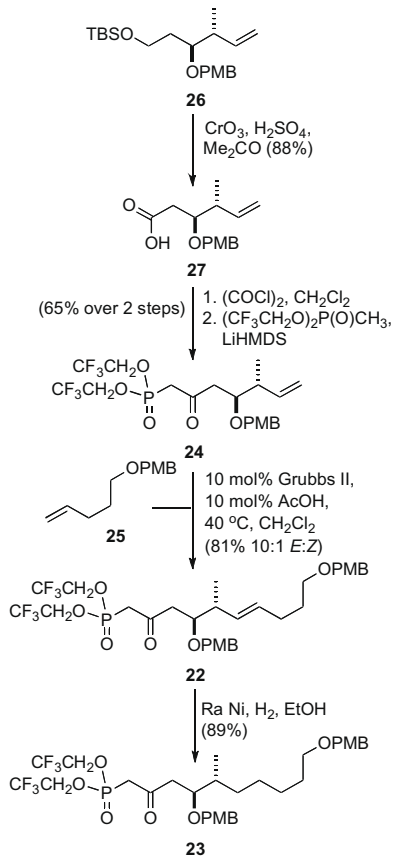

Scheme 5. Synthesis of phosphonates **22** and **23**.

With the two β-ketophosphonates **22** and **23** in hand, the targeted analogues **7** and **8** were then completed in a parallel synthesis sequence (Scheme 6). First the phosphonates were each coupled with the fully elaborated C11–C26 aldehyde **10** under modified Still–Gennari HWE olefination conditions,[18] providing the corresponding (*Z*)-enones, **22** → **28** (65%) and **23** → **29** (54%). DDQ-mediated oxidative cleavage of the C1 and C7 PMB ethers then gave the corresponding triols, **28** → **30** and **29** → **31**. In this situation, the Evans-Saksena hydroxyl-directed reduction proceeded with little or no stereocontrol. As previously observed, a switch to the Corey–Bakshi–Shibata (*R*)-oxazoborolidine-mediated reduction[9f,20] afforded the desired 1,3-*anti* diols, **30** → **32** (95%, 88:12 dr) and **31** → **33** (85%, 89:11 dr), with high diastereoselectivity. The 1,3-diols were then transformed into their acetonides,[28] followed by chemoselective oxidation of the primary alcohol (TEMPO/BAIB; $NaClO_2$) to afford the *seco*-acids, **32** → **34** and **33** → **35**. Finally, macrolactonisation under Yamaguchi conditions proceeded in high yield, and subsequent global deprotection and HPLC purification afforded 2,3-dihydrodictyostatin (**7**, 39%) and 2,3,4,5-tetrahydrodictyostatin (**8**, 45%) in readiness for biological evaluation. Irrespective of the chosen deprotection conditions (HF·pyridine or HCl/MeOH), some translactonisation to the C19 hydroxyl occurred to generate the isodictyostatins[29] (**36**, 28% and **37**, 23%) which were also isolated in the aforementioned HPLC purification. Sufficient material was obtained to allow the additional biological evaluation of these novel 20-membered macrolides.

3. Biological evaluation

The cell growth inhibitory activities of the five novel dictyostatin analogues **6**, **7**, **8**, **36** and **37** were evaluated in vitro relative to

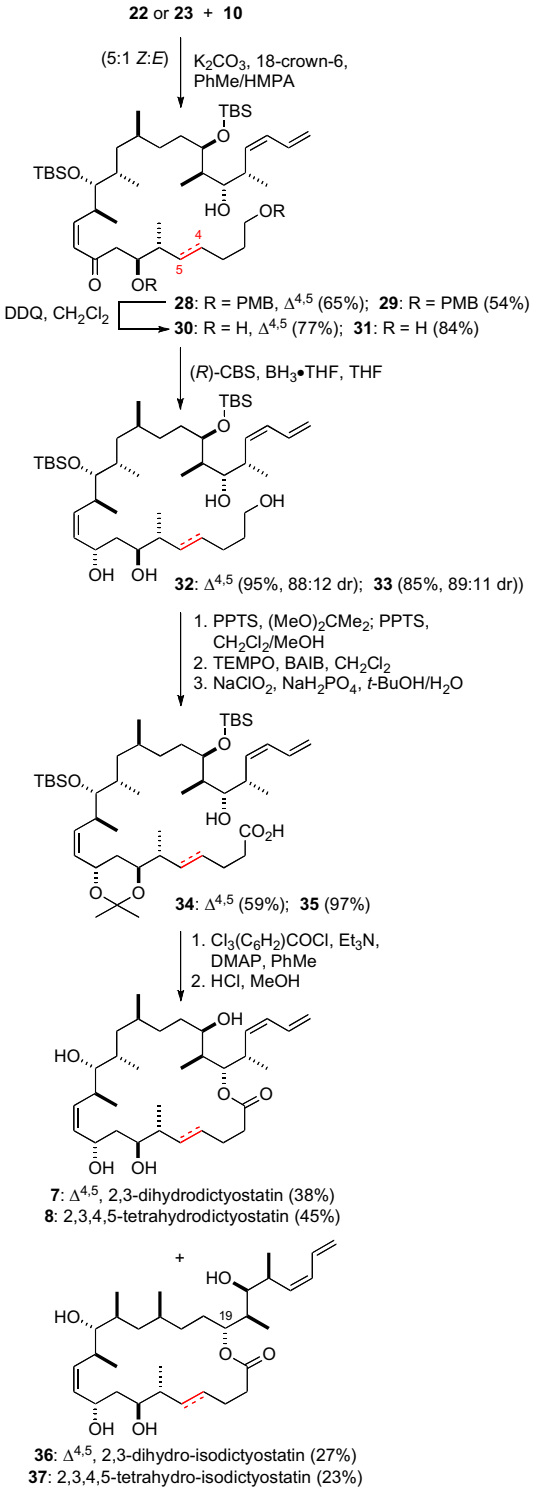

Scheme 6. Completion of the synthesis of 2,3-dihydro- (**7**) and 2,3,4,5-tetrahydrodictyostatin (**8**).

Taxol (**1**), dictyostatin (**4**) and discodermolide (**5**)[9a] against four human cancer cell lines: AsPC-1 (pancreatic), DLD-1 (colon), PANC-1 (pancreatic) and NCI/ADR (Taxol-resistant ovarian) (Table 1).

Drug resistance is mediated in the NCI/ADR cell line by the overexpression of a P-glycoprotein in the cell membrane, facilitating the removal of the drug agent from the cell. A broad spectrum of activities against all four cancer cell lines were shown by our synthetic dictyostatin analogues. As anticipated, 6-desmethyldictyostatin (**6**) displayed low nanomolar cytotoxicity similar to dictyostatin, and notably superior to discodermolide, in both the Taxol-sensitive and resistant cell lines. This result is consistent with the findings of the Curran group,[9e] where 6-*epi*-dicyostatin was found to be essentially equipotent to dictyostatin in its activity against the Taxol-resistant ovarian 1A9/Ptx22 cell line. Moreover, both sets of results are consistent with the C6 substituent being in a relatively open region of the binding site on β-tubulin, where it forms no strong binding interaction. In both the Taxol-sensitive and resistant cell lines, 2,3-dihydrodictyostatin (**7**) and 2,3,4,5-tetrahydrodictyostatin (**8**) showed growth inhibitory activity resembling that of discodermolide, but lower levels relative to dictyostatin. We attribute this to a decreased entropic component of the binding energy as a result of the greater rotational freedom of the C1–C5 region upon partial and complete saturation. As a nanomolar level of antiproliferative activity was still observed for both these analogues against the AsPC-1 (pancreatic), DLD-1 (colon), PANC-1 cell lines, the presence of the (2*Z*)-olefin or (4*E*)-olefin does not appear to be critical. With regard to the isodictyostatin analogues **36** and **37**, a large decrease in cell growth inhibition to micromolar levels was observed upon translactonisation to the 20-membered macrolactone. Presumably, this drastically alters the conformation and reduces the binding energy relative to that of dictyostatin, leading to the dramatic attenuation of antiproliferative activity. In a separate series of incubatory experiments performed on the PANC-1 cell line, the most active analogues, 6-desmethyl- (**6**) and 2,3-dihydrodictyostatin (**7**), were shown to act in an analogous fashion to dictyostatin, through a mechanism of microtubule stabilisation, causing both an accumulation of cells at the G2/M phase (Table 2) and formation of characteristic dense intracellular microtubule bundles (Fig. 5).

Table 1
Growth inhibitory concentrations of analogues **6**, **7**, **8**, **36** and **37** relative to Taxol (**1**), dictyostatin (**4**) and discodermolide (**5**)[9a] against four cultured human cancer cell lines, as determined by MTT metabolism following 72 h exposure to the test agent

Compound	IC_{50}/nM[a]			
	AsPC-1 (pancreatic)	DLD-1 (colon)	PANC-1 (pancreatic)	NCI/ADR (paclitaxel-resistant)
1	89 (±23)	22 (±3.5)	9.9 (±3.6)	1300 (±345)
4	6.2 (±1.7)	2.2 (±0.9)	4.2 (±1.7)	6.6 (±1.0)
5[b]	98 (±34)	29 (±8)	59 (±34)	160 (±34)
6	56 (±25)	8.1 (±3.8)	17 (±10)	43 (±13)
7	94 (±28)	22 (±13)	42 (±7)	66 (±11)
36	3100 (±890)	930 (±580)	1900 (±330)	1600 (±490)
8	120 (±25)	55 (±13)	64 (±33)	130 (±66)
37	4900 (±1100)	1500 (±200)	3200 (±170)	3100 (±790)

[a] Values are ±standard deviation (in parentheses) from a minimum of three experiments.
[b] Data taken from Ref. 9a

4. Conclusions

By adapting our total synthesis, a series of novel C2–C6 modified analogues of the microtubule-stabilising marine natural product dictyostatin were prepared and evaluated in vitro for growth inhibition against a range of human cancer cell lines, including the (P-glycoprotein efflux-mediated) Taxol-resistant NCI/ADR cell line. Removal of the C6 methyl substituent, as in 6-desmethyldictyostatin (**6**), was found to be well tolerated and led to the retention of low nanomolar antiproliferative activity (IC_{50} = 43 nM in the Taxol-resistant NCI/ADR cell line), while partial and full saturation of the (2*Z*,4*E*)-dienoate region in analogues **7** and **8**, respectively, led to a progressive reduction in potency. In contrast, the isomeric 20-membered macrolides **36** and **37** were essentially inactive (micromolar IC_{50}). Notably, 6-des-

Table 2
Cell cycle analysis by flow cytometry of PANC-1 cells incubated for 24 h with ethanol (vehicle control) and 100 nM concentrations of analogues **6**, **7**, **8** and dictyostatin. All three analogues and dictyostatin show an accumulation of cells at the G2/M phase

Compound	% of cells in cell cycle phase			Observations
	G1	S	G2	
Ethanol control	46	33	21	Normal
4	4.2	14	82	G2/M arrest
6	8.0	17	76	G2/M arrest
7	9.0	17	75	G2/M arrest
8	6.0	9.0	84	G2/M arrest

methyldictyostatin (**6**) was the most potent analogue studied, with a cytotoxicity in both Taxol-sensitive and resistant cell lines only slightly less than the parent dictyostatin, and superior to that displayed by discodermolide. The next most active analogue was 2,3-dihydrodictyostatin (**7**), which had an activity resembling that of discodermolide. These new SAR results and that reported for other analogues,[9] combined with consideration of the bioactive conformation of dictyostatin and docking studies,[10] should facilitate the design and synthesis of further simplified dictyostatin analogues that retain a low nanomolar cytotoxicity profile comparable to the natural product.

5. Experimental

5.1. Biological assays

Cytotoxicity assays were conducted using a standard MTT based protocol as described previously.[30] Cell cycle and immunofluorescence imaging of PANC-1 cells were conducted as per protocols described previously.[5]

5.2. General experimental procedures

^{1}H and ^{13}C NMR spectra were recorded in $CDCl_3$, C_6D_6 or CD_3OD on a Bruker Avance BB-ATM, TCI-ATM and DRX-400. IR spectra were measured on a Perkin Elmer Spectrum One (FT-IR) spectrophotometer. HRMS were obtained from the EPSRC Mass Spectrometry Service (Swansea, UK) using a Micromass 0-+-Q-TOF or Bruker Bioapex FT-ICR spectrometer. Optical rotations were recorded on a Perkin Elmer 241 polarimeter and $[\alpha]_D$ values given in 10^{-1} deg cm^2 g^{-1} at a concentration, *c* (g/100 mL). Preparative HPLC on a Varian silica HPLC column (250 mm, 5 μm, flow 1 mL/min) used IPA/hexane (gradients) as solvent, with UV absorption detection at 254 nm and 205 nm. Analytical TLC was carried out on Merck Kieselgel 60 F_{254} plates with visualization using UV (254 nm), potassium permanganate and/or PMA/$Ce(SO_4)_2$ dip. Flash column chromatography was carried out on Merck Kieselgel 60 (230–440 mesh) under a positive pressure. Solvents were redistilled prior to use. Reagents were used as received unless stated otherwise.

5.2.1. 6-Desmethyldictyostatin (6)

To a solution of macrolactone **21** (13 mg, 16 μmol, 1.0 equiv) in THF (1600 μL) was added dropwise HF·pyridine (400 μL) at 0 °C. After warming to room temperature the reaction mixture was stirred for 48 h. The reaction was quenched after cooling to 0 °C by the careful addition of $NaHCO_3$ (1 mL) and the phases separated. The aqueous phase was extracted with EtOAc (3 × 2 mL) and the combined organic extracts dried (Na_2SO_4) and concentrated in vacuo. Flash column chromatography (50% EtOAc/hexane → 100% EtOAc)

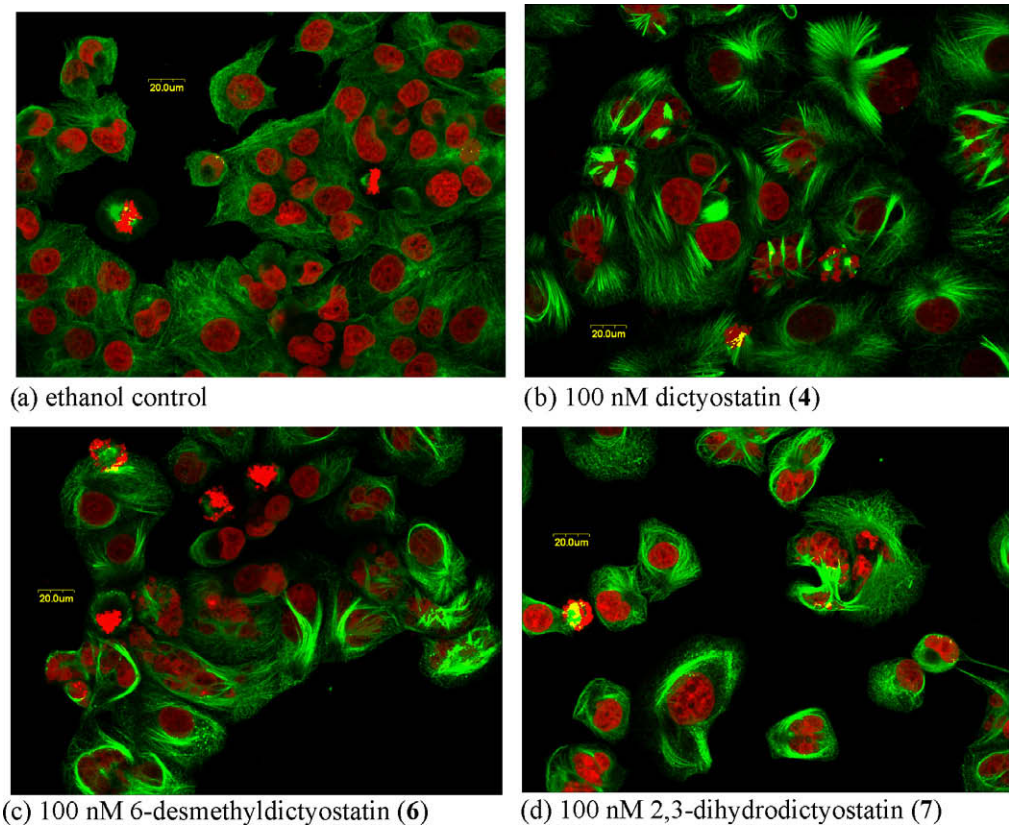

(a) ethanol control (b) 100 nM dictyostatin (**4**)
(c) 100 nM 6-desmethyldictyostatin (**6**) (d) 100 nM 2,3-dihydrodictyostatin (**7**)

Figure 5. Immunofluorescence images of PANC-1 cells stained with anti-α-tubulin (green) and propidium iodide (red) and observed by confocal microscopy. Cells were exposed to ethanol (vehicle control) or 100 nM concentrations of 6-desmethyldictyostatin, 2,3-dihydrodictyostatin or dictyostatin. All three of these compounds show dense microtubule bundles characteristic of microtubule polymerising and stabilising agents.

and HPLC (10% IPA/hexane) afforded 6-desmethyldictyostatin **6** (4.4 mg, 53%) as a colourless solid.

$[\alpha]_D^{20}$ +45.1 (*c* 0.18, $CHCl_3$); IR (liquid film)/cm^{-1} 3384, 2959, 2927, 2855, 1697, 1640, 1600, 1458; ^1H NMR (500 MHz, C_6D_6) δ_H 7.77 (1H, dd, *J* = 11.6, 15.3 Hz, H4), 6.62 (1H, *app* td, *J* = 10.9, 17.1 Hz, H25), 6.22 (1H, *app* t, *J* = 11.4 Hz, H3), 5.95 (1H, *app* t, *J* = 11.0 Hz, H24), 5.70 (1H, ddd, *J* = 7.7, 8.0, 12.8 Hz, H5), 5.55–5.48 (2H, m, H2 + H10), 5.29 (1H, *app* t, *J* = 10.3 Hz, H23), 5.27 (1H, *app* t, *J* = 10.9 Hz, H11), 5.10–5.05 (2H, m, H21 + H26a), 5.01 (1H, *br* d, *J* = 10.2 Hz, H26b), 4.74 (1H, *app* q, *J* = 8.4 Hz, H9), 4.00–3.94 (1H, m, H7), 3.68–3.61 (1H, m, OH), 3.32–3.26 (1H, m, H19), 3.25–3.21 (1H, m, H13), 3.06–3.01 (1H, m, OH), 2.98–2.90 (1H, m, H22), 2.74–2.66 (1H, m, H12), 2.29–2.20 (1H, m, H6a), 2.20–2.11 (1H, m, H6b), 2.02–1.96 (1H, m, H15a), 1.81–1.66 (4H, m, H8a + H8b + H14 + H20), 1.63–1.55 (1H, m, H18a), 1.54–1.47 (1H, m, H18b), 1.45–1.16 (3H, m, H16 + H17a + H17b), 1.08 (3H, d, *J* = 6.7 Hz, CH_3-20), 0.98 (3H, d, *J* = 6.9 Hz, CH_3-14), 0.93–0.86 (1H, m, H15b), 0.89 (3H, d, *J* = 6.7 Hz, CH_3-16), 0.83 (3H, d, *J* = 6.7 Hz, CH_3-22), 0.82 (3H, d, *J* = 6.5 Hz, CH_3-12); ^{13}C NMR (125 MHz, C_6D_6) δ_C 166.5 (C1), 146.3 (C3), 142.0 (C5), 134.7 (C23), 134.4 (C11), 133.8 (C10), 132.6 (C25), 130.4 (C24), 129.3 (C4), 117.9 (C26), 115.8 (C2), 76.1 (C21), 75.3 (C13), 73.0 (C19), 67.7 (C7), 66.3 (C9), 44.3 (C8), 40.7 (C6), 40.3 (C15), 39.6 (C14), 35.8 (C22), 35.6 (C12), 32.2 (C20), 32.01 (C17 or C18), 31.96 (C17 or C18), 29.3 (C16), 21.4 (Me16), 17.4 (Me22), 17.3 (Me12), 14.2 (Me14), 10.3 (Me20); HRMS (ESI^+) Calcd for $C_{31}H_{50}O_6Na$ $[M+Na]^+$ 541.3479, found 541.3500; R_f 0.80 (80% EtOAc/hexane); R_t 21.2 min (10% IPA/hexane).

5.2.2. 2,3-Dihydrodictyostatin (7)

To a solution of the protected macrolactone precursor in Scheme 6 (6.9 mg, 8.6 μmol, 1.0 equiv) in MeOH (600 μL) at 0 °C was added a premixed solution of 3N HCl (300 μL) and MeOH (900 μL). After warming slowly to room temperature, the reaction was stirred for 16 h, before being diluted with H_2O (2 mL) and EtOAc (2 mL). The phases were separated, the organic phase extracted with EtOAc (3 × 2 mL) and the combined organic extracts dried (Na_2SO_4) and concentrated in vacuo. The crude material was purified using HPLC (5% IPA/hexane) to yield 2,3-dihydrodictyostatin **7** (1.8 mg, 39%) and 2,3-dihydro-isodictyostatin **36** (1.3 mg, 28%) as colourless solids.

$[\alpha]_D^{20}$ +10.6 (*c* 0.15, $CHCl_3$); IR (liquid film)/cm^{-1} 3364, 2957, 2924, 2854, 1715, 1660, 1633, 1457; ^1H NMR (500 MHz, C_6D_6) δ_H 6.65 (1H, *app* td, *J* = 10.4, 16.6 Hz, H25), 6.00 (1H, *app* t, *J* = 11.0 Hz, H24), 5.61 (1H, dd, *J* = 8.1, 10.9 Hz, H10), 5.35–5.28 (3H, m, H4 + H5 + H23), 5.18 (1H, dd, *J* = 1.7, 9.1 Hz, H21), 5.09 (1H, dd, *J* = 2.0, 16.6 Hz, H26a), 5.04 (1H, *app* t, *J* = 10.9 Hz, H11), 5.00 (1H, *br* d, *J* = 10.3 Hz, H26b), 4.75–4.70 (1H, m, H9), 3.71 (1H, *br* dd, *J* = 2.6, 10.5 Hz, H7), 3.52–3.47 (1H, m, H19), 3.07 (1H, dd, *J* = 2.7, 7.7 Hz, H13), 2.95–2.86 (1H, m, H22), 2.61 (1H, m, H12), 2.45–2.29 (3H, m, H2a + H2b + H3a), 2.25–2.13 (2H, m, H3b + OH), 2.13–2.06 (1H, m, OH), 2.05–1.97 (1H, m, H6), 1.79–1.63 (5H, m, H8a + H14 + H15a + H18a + H20), 1.62–1.56 (1H, m, H16), 1.52 (1H, ddd, *J* = 1.7, 7.6, 14.2 Hz, H8b), 1.47–1.17 (3H, m, H17a + H17b + H18b), 1.05 (3H, d, *J* = 6.8 Hz, CH_3-20), 0.98 (3H, d, *J* = 6.9 Hz, CH_3-6), 0.90 (6H, *app* d, *J* = 6.5 Hz, CH_3-14 + CH_3-16), 0.82 (3H, d, *J* = 6.6 Hz, CH_3-22), 0.80 (3H, d, *J* = 6.5 Hz, CH_3-12), 0.76–0.70 (1H, m, H15b); ^{13}C NMR (125 MHz, C_6D_6) δ_C 173.0 (C1), 136.1 (C10), 135.3 (C23), 133.0 (C11), 132.8 (C25), 132.5 (C5), 130.2 (C4), 130.0 (C24), 117.7 (C26), 76.0 (C21), 74.9 (C13), 74.1 (C19), 71.9 (C7), 66.3 (C9), 43.5 (C6), 41.8 (C8), 40.3 (C20), 40.1 (C15), 36.6 (C12), 35.6 (C16 + C22), 34.6 (C17), 34.0 (C2), 31.7 (C14), 31.1 (C18), 28.1 (C3), 21.2 (Me16), 17.4 (Me22), 17.3 (Me12), 16.1 (Me6), 14.5 (Me14), 9.6 (Me20); HRMS (ESI^+) Calcd for $C_{32}H_{54}O_6Na$ $[M+Na]^+$ 557.3818, found 557.3835; R_f 0.57 (80% EtOAc/hexane); R_t 16.3 min (5% IPA/hexane).

5.2.3. 2,3-Dihydro-isodictyostatin (36)

$[\alpha]_D^{20}$ −1.3 (*c* 0.11, $CHCl_3$); IR (liquid film)/cm^{-1} 3360, 2957, 2923, 2853, 1715, 1660, 1633, 1467; ^1H NMR (500 MHz, C_6D_6) δ_H 6.75 (1H, *app* dtd, *J* = 1.0, 10.6, 16.6 Hz, H25), 6.06 (1H, *app* t, *J* = 11.0 Hz, H24), 5.63 (1H, dd, *J* = 9.5, 10.6 Hz, H10), 5.52–5.48 (1H, m, OH), 5.38–5.34 (1H, m, H19), 5.33–5.25 (3H, m, H4 + H5 + H23), 5.20 (1H, *app* t, *J* = 10.8 Hz, H11), 5.13 (1H, dd, *J* = 2.0, 16.8 Hz, H26a), 5.06 (1H, *br* d, *J* = 10.3 Hz, H26b), 4.77–4.72 (1H, m, H9), 3.75 (1H, ddd, *J* = 2.6, 4.8, 10.3 Hz, H7), 3.36 (1H, dd, *J* = 4.2, 6.6 Hz, H21), 3.13 (1H, dd, *J* = 3.9, 7.2 Hz, H13), 2.93–2.84 (1H, m, H22), 2.64–2.55 (1H, m, H12), 2.37–2.30 (1H, m, H3a), 2.27 (1H, *app* d, *J* = 6.2 Hz, H2a), 2.26 (1H, *app* d, *J* = 7.1 Hz, H2b), 2.18–2.06 (2H, m, H3b + OH), 2.06–2.00 (1H, m, H6), 1.88–1.82 (1H, m, H20), 1.79–1.56 (6H, m, H8a + H8b + H14 + H16 + H18a + H18b), 1.42–1.15 (4H, m, H15a + H15b + H17a + H17b), 1.07 (3H, d, *J* = 7.0 Hz, CH_3-20), 0.98 (3H, d, *J* = 7.0 Hz, CH_3-6), 0.91 (3H, d, *J* = 6.6 Hz, CH_3-16), 0.89 (6H, *app* d, *J* = 6.7 Hz, CH_3-14 + CH_3-22), 0.85 (3H, d, *J* = 6.6 Hz, CH_3-12); ^{13}C NMR (125 MHz, C_6D_6) δ_C 173.1, 135.0, 134.5, 133.5, 133.1, 132.8, 131.1, 130.2, 118.2, 76.6, 76.5, 75.5, 72.2, 66.0, 43.7, 41.8, 38.1, 36.41, 36.38, 34.0, 33.4, 30.4, 30.17, 30.16, 28.3, 20.4, 17.7, 17.6, 15.9, 15.1, 8.4; HRMS (ESI^+) Calcd for $C_{32}H_{54}O_6Na$ $[M+Na]^+$ 557.3818, found 557.3840; R_f 0.45 (80% EtOAc/hexane); R_t 25.6 min (5% IPA/hexane).

5.2.4. 2,3,4,5-Tetrahydrodictyostatin (8)

To a solution of the protected macrolactone precursor in Scheme 6 (6.6 mg, 8.2 μmol, 1.0 equiv) in MeOH (1 mL) at 0 °C was added a premixed solution of 3 N HCl (500 μL) and MeOH (2.2 mL). After slowly warming to room temperature the reaction was stirred for 18 h, before dilution with water (2 mL) and EtOAc (2 mL). The phases were separated, the aqueous phase extracted with EtOAc (3 × 2 mL) and the combined organic extracts dried (Na_2SO_4) and concentrated in vacuo. Flash column chromatography (60% EtOAc/hexane) afforded a mixture of 2,3,4,5-tetrahydrodictyostatin **8** and 2,3,4,5-tetrahydro-isodictyostatin **37** (3.0 mg, 1.5:1 **8**:**37**, 75%) which were subsequently separated using HPLC (5% IPA/hexane) affording **8** (1.9 mg, 45%) and **37** (1.0 mg, 23%) as colourless solids.

$[\alpha]_D^{20}$ +17.6 (*c* 0.13, $CHCl_3$); IR (liquid film)/cm^{-1} 3385, 2961, 2925, 2856, 1715, 1668, 1460; ^1H NMR (500 MHz, C_6D_6) δ_H 6.66 (1H, *app* dtd, *J* = 1.0, 10.5, 17.0 Hz, H25), 6.00 (1H, *app* t, *J* = 11.0 Hz, H24), 5.65 (1H, dd, *J* = 8.0, 11.1 Hz, H10), 5.33 (1H, *app* t, *J* = 11.0 Hz, H23), 5.19 (1H, dd, *J* = 1.8, 8.9 Hz, H21), 5.12 (1H, dd, *J* = 2.0, 16.9 Hz, H26a), 5.10 (1H, *app* dt, *J* = 1.1, 11.1 Hz, H11), 5.02 (1H, *br* d, *J* = 10.0 Hz, H26b), 4.70–4.64 (1H, m, H9), 3.80 (1H, *br* d, *J* = 10.5 Hz, H7), 3.44–3.38 (1H, m, H19), 3.07 (1H, dd, *J* = 2.1, 8.1 Hz, H13), 2.95–2.86 (1H, m, H22), 2.54–2.46 (1H, m, H12), 2.32 (1H, ddd, *J* = 6.2, 9.5, 15.7 Hz, H2a), 2.23 (1H, ddd, *J* = 7.0, 13.1, 16.6 Hz, H2b), 2.16–1.93 (1H, *br* s, OH), 1.79–1.65 (5H, m, H3a + H8a + H14 + H15a + H20), 1.64–1.50 (4H, m, H3b + H8b + H16 + H18a), 1.45–1.30 (7H, m, H4a + H5a + H5b + H6 + H17a + H17b + H18b), 1.26–1.19 (1H, m, H4b), 1.02 (3H, d, *J* = 7.1 Hz, CH_3-20), 0.90 (3H, d, *J* = 6.6 Hz, CH_3-16), 0.87 (6H, *app* d, *J* = 6.9 Hz, CH_3-6 + CH_3-14), 0.82 (3H, d, *J* = 6.7 Hz, CH_3-22), 0.79 (3H, d, *J* = 6.7 Hz, CH_3-12), 0.84 (1H, *app* t, *J* = 9.1 Hz, H15b); ^{13}C NMR (125 MHz, C_6D_6) δ_C 173.6 (C1), 135.5 (C10), 135.2 (C23), 133.1 (C11), 132.8 (C25), 130.0 (C24), 117.7 (C26), 75.5 (C21), 75.0 (C13), 74.4 (C19), 71.9 C(7), 67.4 (C9), 40.7 (C20), 39.9 (C6), 39.2 (C15), 38.9 (C8), 36.4 (C12), 35.6 (C22), 35.2 (17), 34.4 (C2), 32.1 (C4), 31.7 (C14), 31.1 (C18), 29.3 (C16), 26.8 (C5), 25.4 (C3), 21.2 (Me16), 17.4 (Me22), 17.3 (Me12), 15.2 (Me6), 14.4 (Me14), 10.0 (Me20); HRMS (ESI^+) Calcd for $C_{32}H_{56}O_6Na$ $[M+Na]^+$ 559.3975, found 559.3948; R_f 0.37 (80% EtOAc/hexane); R_t 22.4 (5% IPA/hexane).

5.2.5. 2,3,4,5-Tetrahydro-isodictyostatin (37)

$[\alpha]_D^{20}$ +8.5 (*c* 0.06, $CHCl_3$); IR (liquid film)/cm^{-1} 3361, 2961, 2924, 2854, 1715, 1663, 1634, 1460; ^1H NMR (500 MHz, C_6D_6) δ_H 6.72 (1H, *app* dtd, *J* = 0.9, 10.5, 16.8 Hz, H25), 6.03 (1H, *app* t, *J* = 10.8 Hz, H24), 5.62 (1H, dd, *J* = 9.1, 11.1 Hz, H10), 5.52–5.48 (1H, m, OH), 5.33 (1H, *app* td, *J* = 5.3, 7.9 Hz, H19), 5.24 (1H, *app* t, *J* = 10.8 Hz, H11), 5.21 (1H, *app* t, *J* = 10.2 Hz, H23), 5.12 (1H, dd, *J* = 1.8, 16.6 Hz, H26a), 5.04 (1H, *br* d, *J* = 10.3 Hz, H26b), 4.69–4.63 (1H, m, H9), 3.85 (1H, *br* dd, *J* = 3.8, 9.7 Hz, H7), 3.29 (1H, *app* td, *J* = 3.9, 7.1 Hz, H21), 3.02 (1H, dd, *J* = 4.4, 6.6 Hz, H13), 2.92–2.84 (1H, m, H22), 2.53–2.46 (1H, m, H12), 2.30 (1H, *app* td, *J* = 8.0, 15.4 Hz, H2a), 2.23 (1H, ddd, *J* = 6.5, 8.0, 15.3 Hz, H2b), 2.13–2.06 (2H, m, 2 × OH), 1.88–1.82 (1H, m, H20), 1.80–1.70 (2H, m, H8a + H18a), 1.67–1.42 (9H, m, H3a + H3b + H6 + H8b + H14 + H15a + H15b + H16 + H18b), 1.40–1.10 (6H, m, H4a + H4b + H5a + H5b + H17a + H17b), 1.06 (3H, d, *J* = 6.7 Hz, CH_3-20), 0.89 (3H, d, *J* = 7.0 Hz, CH_3-16), 0.86 (3H, d, *J* = 7.1 Hz, CH_3-14), 0.85 (6H, *app* d, *J* = 6.9 Hz, CH_3-6 + CH_3-22), 0.83 (3H, d, *J* = 6.7 Hz, CH_3-12); ^{13}C NMR (125 MHz, C_6D_6) δ_C 173.3, 134.6, 134.3, 132.8, 132.7, 131.0, 118.4, 76.5, 76.1, 75.7, 71.8, 66.9, 41.5, 38.7, 38.5, 36.2, 34.2, 32.9, 31.9, 30.7, 30.2, 29.7, 29.6, 29.5, 27.7, 26.1, 25.3, 20.3, 17.7, 17.5, 14.7, 9.1; HRMS (ESI^+) Calcd for $C_{32}H_{56}O_6Na$ $[M+Na]^+$ 559.3975, found 559.3948; R_f 0.18 (50% EtOAc/hexane); R_t 31.7 min (5% IPA/hexane).

Acknowledgements

NIH Grant No. CA-93455 provided financial support for the biological assays and general project support was provided by the EPSRC and AstraZeneca (CASE studentship to N.M.G.). We thank Professor John Leonard (AstraZeneca) for helpful discussions, Dr. J. Fernando Diaz (CSIC, Madrid) for providing AutoDock 3D structures, Ms. Tara Pitts (HBOI) and Ms. Pat Linley (HBOI) for assistance in our biological evaluation, Samantha Cheung (Cambridge) for some preliminary synthetic studies and Dr. Stuart Mickel (Novartis) for the gift of chemicals.

Supplementary data

Supplementary data associated with this article, including full experimental details for intermediates and copies of NMR spectra of analogues prepared can be found, in the online version, at doi:10.1016/j.bmc.2008.10.084.

References and notes

1. Bergstralh, D. T.; Ting, J. P. Y. *Cancer Treat. Rev.* **2006**, *32*, 166; Kavallaris, M.; Verrills, N. M.; Hill, B. T. *Drug Resist. Updat.* **2001**, *4*, 392; Kuppens, I. E. L. M. *Curr. Clin. Pharmacol.* **2006**, *1*, 57.
2. Altmann, K. H.; Gertsch, J. *Nat. Prod. Rep.* **2007**, *24*, 327.
3. http://www.fda.gov/bbs/topics/NEWS/2007/NEW01732.html.
4. Pettit, G. R.; Cichacz, Z. A.; Gao, F.; Boyd, M. R.; Schmidt, J. M. *J. Chem. Soc., Chem. Commun.* **1994**, *9*, 1111.
5. Isbrucker, R. A.; Cummins, J.; Pomponi, S. A.; Longley, R. E.; Wright, A. E. *Biochem. Pharmacol.* **2003**, *66*, 75.
6. Paterson, I.; Britton, R.; Delgado, O.; Wright, A. E. *Chem. Commun.* **2004**, 632.
7. (a) Paterson, I.; Britton, R.; Delgado, O.; Meyer, A.; Poullennec, K. G. *Angew. Chem. Int. Ed.* **2004**, *43*, 4629; (b) Shin, Y.; Fournier, J. H.; Fukui, Y.; Bruckner, A. M.; Curran, D. P. *Angew. Chem. Int. Ed.* **2004**, *43*, 4634; (c) Shin, Y.; Fournier, J. H.; Bruckner, A.; Madiraju, C.; Balachandran, R.; Raccor, B. S.; Edler, M. C.; Hamel, E.; Sikorski, R. P.; Vogt, A.; Day, B. W.; Curran, D. P. *Tetrahedron* **2007**, *63*, 8537.
8. (a) Madiraju, C.; Edler, M. C.; Hamel, E.; Raccor, B. S.; Balachandran, R.; Zhu, G.; Giuliano, K. A.; Vogt, A.; Shin, Y.; Fournier, J. H.; Fukui, Y.; Brückner, A. M.; Curran, D. P.; Day, B. W. *Biochemistry* **2005**, *44*, 15053; (b) Buey, R. M.; Barasoain, I.; Jackson, E.; Meyer, A.; Giannakakou, P.; Paterson, I.; Mooberry, S.; Andreu, J. M.; Diaz, J. F. *Chem. Biol.* **2005**, *12*, 1269.
9. (a) Paterson, I.; Gardner, N. M.; Poullennec, K. G.; Wright, A. E. *Bioorg. Med. Chem. Lett.* **2007**, *17*, 2443; (b) Shin, Y.; Fournier, J. H.; Balachandran, R.; Madiraju, C.; Raccor, B. S.; Zhu, G.; Edler, M. C.; Hamel, E.; Day, B. W.; Curran, D. P. *Org. Lett.* **2005**, *7*, 2873; (c) Paterson, I.; Gardner, N. M.; Poullennec, K. G.; Wright, A. E. *J. Nat. Prod.* **2008**, *71*, 364; (d) Shin, Y.; Choy, N.; Balachandran, R.; Madiraju, C.; Day, B. W.; Curran, D. P. *Org. Lett.* **2002**, *4*, 4443; (e) Fukui, Y.; Bruckner, A. M.; Shin, Y.; Balachandran, R.; Day, B. W.; Curran, D. P. *Org. Lett.* **2006**, *8*, 301; (f) Paterson, I.; Gardner, N. M. *Chem. Commun.* **2007**, 49; (g) Jung, W. H.; Harrison, C.; Shin, Y.; Fournier, J. H.; Balachandran, R.; Raccor, B. S.; Sikorski, R. P.; Vogt, A.; Curran, D. P.; Day, B. W. *J. Med. Chem.* **2007**, *50*, 2951; (h) Raccors, B. S.; Vogt, A.; Sikorski, R. P.; Madiraju, C.; Balachandran, R.; Montgomery, K.; Shin, Y.; Fukui, Y.; Jung, W. H.; Curran, D. P.; Day, B. W. *Mol. Pharmacol.* **2008**, *73*, 718.
10. Canales, A.; Matesanz, R.; Gardner, N. M.; Andreu, J. M.; Paterson, I.; Díaz, F.; Jiménez-Barbero, J. *Chem. Eur. J.* **2008**, *14*, 7557.
11. (a) Florence, G. J.; Gardner, N. M.; Paterson, I. *Nat. Prod. Rep.* **2008**, *25*, 342; (b) Paterson, I.; Florence, G. J. *Eur. J. Org. Chem.* **2003**, 2193; (c) Smith, A. B., III.; Freeze, S. B. *Tetrahedron* **2008**, *64*, 261.
12. For a preliminary account of this work, See: Paterson, I.; Gardner, N. M.; Guzman, E.; Wright, A. E. *Biorg. Med. Chem. Lett.* **2008**, *18*. doi:10.1016/j.bmcl.2008.09.109.
13. Ficini, J.; Claude, B.; Desmaele, D.; Ouerfelli, O. *Heterocycles* **1987**, *25*, 329.
14. Schlaus, S. E.; Brandes, B. D.; Larrow, J. F.; Tokunaga, M.; Hansen, K. B.; Gould, A. E.; Furrow, M. E.; Jacobsen, E. N. *J. Am. Chem. Soc.* **2002**, *124*, 1307.
15. The enantiomeric excess was determined by ^1H NMR analysis of the Mosher ester derivatives of alcohol **15**.
16. Takai, K.; Nitta, K.; Utimoto, K. *J. Am. Chem. Soc.* **1986**, *108*, 7408.
17. Devos, A.; Remion, J.; Frisque-Hesbain, A. M.; Colens, A.; Ghosez, L. *J. Chem. Soc., Chem. Commun.* **1979**, 1180.
18. Still, W. C.; Gennari, C. *Tetrahedron Lett.* **1983**, *24*, 4405; Paterson, I.; Lyothier, I. *Org. Lett.* **2004**, *6*, 4933.
19. Evans, D. A.; Chapman, K. T.; Carreira, E. M. *J. Am. Chem. Soc.* **1988**, *110*, 3560.
20. Corey, E. J.; Bakshi, R. K.; Shibata, S. *J. Am. Chem. Soc.* **1987**, *109*, 5551.
21. Allred, G. D.; Liebeskind, L. S. *J. Am. Chem. Soc.* **1996**, *118*, 2748.
22. Inanaga, J.; Hirata, K.; Saeki, H.; Katsuki, T.; Yamaguchi, M. *Bull. Chem. Soc. Jpn.* **1979**, *52*, 1989.
23. Attempts to model the conformational effects of saturation of the C1–C5 region relative to the global energy minimum conformer of dictyostatin (Ref. 6) were complicated by the increased degree of rotational freedom associated with the C2–C5 carbon chain.
24. Bowden, K.; Heilbron, I. M.; Jones, E. R. H. *J. Chem. Soc.* **1946**, 39.
25. Chatterjee, A. K.; Choi, T. L.; Sanders, D. P.; Grubbs, R. H. *J. Am. Chem. Soc.* **2003**, *125*, 11360.
26. Hong, S. H.; Sanders, D. P.; Lee, C. W.; Grubbs, R. H. *J. Am. Chem. Soc.* **2005**, *127*, 17160.
27. Without the AcOH additive, the cross-metathesis reaction proceeded only in low yield (ca. 10%). It is proposed that the in situ generation of ruthenium hydride facilitates olefin isomerisation, preventing the metathesis proceeding. See: Hong, S. H.; Wenzel, A. G.; Salguero, T. T.; Day, M. W.; Grubbs, R. H. *J. Am. Chem. Soc.* **2007**, *129*, 7961.
28. During the course of acetonide protection, the primary C1 alcohol formed a mixed acetal which was cleaved selectively (PPTS, CH_2Cl_2 and MeOH) before the oxidation sequence.
29. Translactonisation has been avoided previously by employing anhydrous deprotection conditions using HF·pyridine. The increased reactivity of the saturated lactones to transacylation may be responsible for the reappearance of these isodictyostatin by-products.
30. Gunasekera, S. P.; Zuleta, I. A.; Longley, R. E.; Wright, A. E.; Pomponi, S. A. *J. Nat. Prod.* **2003**, *66*, 1615.